Proceedings of the IASTED International Conference
ROBOTICS AND MANUFACTURING
July 26-29, 1998, Banff, Canada

Evaluation on Transition Stability of Enveloped Objects Using Force-flow Diagram

Makoto Kaneko Mitsuru Higashimori Kensuke Harada Toshio Tsuji

Industrial and Systems Engineering
Hiroshima University
Kagamiyama Higashi-Hiroshima 739, Japan

Abstract

This paper discusses the transition stability in sliding an object enveloped by a multi-fingered robot hand whose joints are under constant torque command. We provide a concept on transition stability, where a transition is called stable if the object is guaranteed to reach the goal section without moving away from a virtual cylinder defined in hand working space. We evaluate the transition stability by using force-flow diagram, where we can observe the global moving direction of object without solving the differential equation with respect to time. Through such force-flow diagram, it is shown that the transition phase becomes stable for a concave object while it becomes unstable for a convex object.

Key words: *Enveloping grasp, Grasp transition, Grasp stability, Constant torque control, Force-flow diagram.*

1 Introduction

There have been a number of works concerning multi-fingered robot hand. Most of them address finger tip grasps. For this type of grasp, we can emphasize on dexterity and sensitivity. Enveloping grasp (or power grasp) provides another grasping style, where multiple contacts between one finger and the object are allowed. Such an enveloping grasp can support a large load in nature and is highly stable due to a large number of distributed contacts on the grasped object. While there are still many works in enveloping grasps, most of them discuss the contact force analysis [1]-[3], robustness of grasp [4], [5] and so forth, by implicitly assuming that the grasped object does not move.

On the other hand, we are particularly interested in the whole grasping procedure as shown in Fig.1, where the hand first approaches an object placed on a table (approach phase) and lifts up the object toward the palm (lifting phase) until an enveloping grasp (grasping phase) is completed [6]-[8]. In this paper, we focus on the final part of the lifting phase, where the object is still moving toward the palm. The motion planning of object in this phase can be regarded as an issue for manipulating an object enveloped by finger links. However, since contact forces can not be described explicitly, it is hard to determine the exact trajectory of object. In the lifting phase, fortunately, we do not care the exact trajectory of object, because the purpose is to simply move the object to the palm. We call such sliding phase transition phase in terminology. Under constant torque commands, can we always achieve a stable transition from an arbitrary point to the palm without dropping the object from hand? This work is motivated by such a question.

We begin by introducing a concept of transition stability [9]. The basic idea of this definition is as follows. For example, let us consider a virtual pipe in the hand working space. If an object is moved from one section to another without away from the surface of the pipe, we regard that the transition is stable in a global sense. This concept perfectly matches with the lifting phase since the goal is to convey the object to the palm without dropping the object from the hand. To utilize this concept, we introduce the force-flow which is a convenient tool for judging whether the object motion in designated direction is realized or not. The force-flow-diagram is defined by the map displaying the force-flow at various position of the center of gravity of object. This diagram visually tells us a rough behaviour of object during a transition phase without solving any differential equations with respect to time. Additionally, this diagram provides us with an important information on the behaviour of object against a disturbance in the grasping phase. In conventional works, the robustness of enveloping grasps has been evaluated by the maximum external force and moment which can resist without sliding [1], [4] or by the volume of the convex polygon spanned by external force and moment that can resist without changing joint torques [5]. However, even though the object makes some slip due to an external disturbance, we can regard it stable in a global sense if the object comes back to the neighborhood of the original position after removing the disturbance.

For various objects, we examine the transition stability by utilizing the force-flow diagram and show that the transition phase tends to be stable for a concave object,

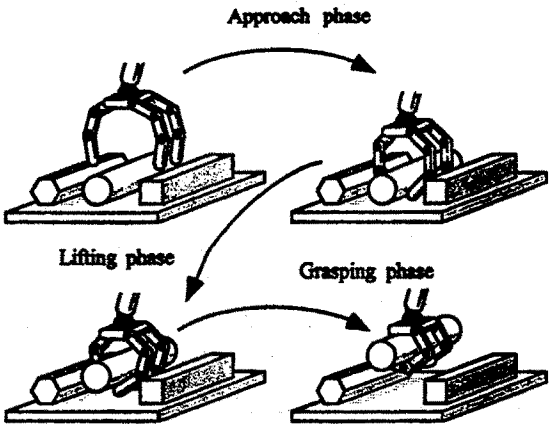

Fig.1 An example of enveloping grasp

while it becomes unstable for a convex object, such as sphere.

2 Related work

Approach phase:
Jeannerod[10] has studied human grasping intensively and has shown that during the approaching phase of grasping, the hand preshapes in order to prepare the shape matching with the object to be grasped. Bard and Troccaz[11] introduced such a preshaping motion into a robotic hand by utilizing low-level visual data.

Lifting phase:
Trinkle and Paul[12] proposed the concept of grasp liftability and derived the liftability regions of a frictionless planar object for use in manipulation planning.

grasping phase:
Mirrza and Orin [1] applied a linear programming approach to formulate and solve the force distribution problem in power grasps, and showed a significant increase in the maximum weight handling capability for completely enveloping type power grasps. Trinkle [13] analyzed planning techniques for enveloping, and frictionless grasping. Salisbury [14] has proposed the Whole-Arm Manipulation (WAM) capable of treating a big and heavy object by using one arm which allows multiple contacts with an object. Bicchi [2] showed that internal forces in power grasps which allow inner link contacts can be decomposed into active and passive ones. Omata and Nagata [3] analyzed the indeterminate grasp force by considering that contact sliding directions are constrained in power grasps. Zhang et. al.[4] evaluated the robustness of power grasp by utilizing the virtual work rate for all virtual displacements.

Work combined with more than two phases:
For a two-fingered hand whose opening is controlled by a single parameter, Rimon and Blake [15] discussed a preshaping problem combining with the grasping phase. Kleinmann et. al.[16] showed a couple of approaches for finally achieving a power grasp from a finger tip grasp. In our previous work [6], we have shown that human chooses the grasp planning according to the scale of objects, even though they are geometrically similar (Scale-Dependent Grasp). Based on the observation of

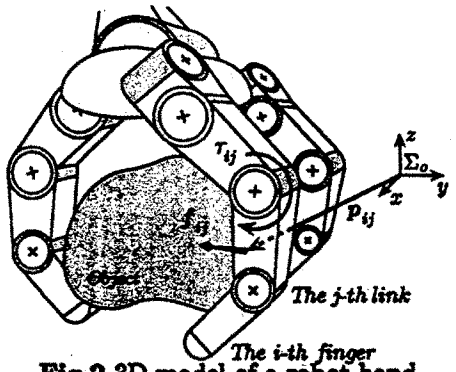

Fig.2 3D model of a robot hand

human grasping, we introduced three grasping strategies depending upon the size of objects for cylindrical objects placed on a table [7],[8].

3 Sliding Condition for an Enveloped Object

Between the lifting and the grasping phases, an enveloped object slides over link surface until it reaches the palm. However, if the lifting force balances with the gravitational force, the object will stop before reaching the palm. Whether the object stops before reaching the palm or not depends on how much torque command is imparted to each joint. In this chapter, we first formulate the relationship between torque and contact force, and then consider a sufficient condition leading to sliding motion.

3.1 Assumptions

To simplify the discussion, we set the following assumptions:

- Assumption 1: The robot finger has m fingers and n joints per finger.
- Assumption 2: The mass of finger link is negligible.
- Assumption 3: At each contact, we assume a Coulomb friction whose coefficient is given by μ, where both static and dynamic frictional coefficients are not distinguished.
- Assumption 4: Interference among fingers is ignored.
- Assumption 5: Each joint has a joint position sensor and a joint torque sensor.
- Assumption 6: Each link has at least one contact with the object.
- Assumption 7: The motion is slow enough to suppress any dynamic effect.

3.2 Relationship between torque and contact force

Let us consider the ith finger of the robot hand as shown in Fig.2. $p_{ij} \in \mathcal{R}^{3\times1}$, $f_{ij} \in \mathcal{R}^{3\times1}$ and $\tau_i \in \mathcal{R}^{n\times1}$ denote the contact position vector, the contact force vector, and the joint torque vector, respectively, where i and j express the ith finger and the jth contact point, respectively.

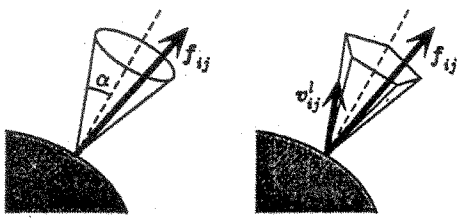

(a) friction cone (b) polyhedral convex cone

Fig.3 Friction cone and its model

Let τ_i^j be the torque vector due to the contact force $f_{i,j}$. τ_i^j is given by

$$\tau_i^j = J_{ij}^{\mathrm{T}} f_{ij} \tag{1}$$

where J_{ij}^T denotes the transpose of Jacobean matrix which maps the contact force into the joint torque. By utilizing the principle of superposition for the relationship between τ_i^j and f_{ij}, we can obtain

$$\tau_i = \sum_{j=1}^{k_i} \tau_i^j \tag{2}$$

$$= \sum_{j=1}^{k_i} J_{ij}^{\mathrm{T}} f_{ij} \tag{3}$$

where k_i denotes the number of the contact point of the ith finger. Eq.(3) is rewritten in the following form.

$$\tau_i = J_i^{\mathrm{T}} f_i \tag{4}$$

where

$$J_i^{\mathrm{T}} = \left[J_{i1}^{\mathrm{T}}, \ldots, J_{ik_i}^{\mathrm{T}}\right] \in \mathcal{R}^{n \times 3k_i} \tag{5}$$

$$f_i = \left[f_{i1}^T, \ldots, f_{ik_i}^T\right]^T \in \mathcal{R}^{3k_i \times 1} \tag{6}$$

Eq.(4) expresses the relationship between the contact force and the joint torque in ith finger. A contact force always appears within a friction cone as shown in Fig.3(a), where $\alpha = \tan^{-1}\mu$. In practice, the friction cone can be approximated by a polyhedral convex cone generated by a finite set of vectors (Fig.3(b)) such that we can obtain a set of linear equations [5]. Force set within the cone is represented by

$$f_{ij} = \sum_{l=1}^{L} \lambda_{ij}^l v_{ij}^l \qquad (\lambda_{ij}^l \geq 0) \tag{7}$$

where v_{ij}^l is the unit vector directing lth edge line. Note that in general the vectors v_{ij}^l are not linearly independent. Eq.(7) can be rewritten into the following form.

$$f_{ij} = V_{ij} \lambda_{ij} \tag{8}$$

where

$$V_{ij} = [v_{ij}^1, \ldots, v_{ij}^L] \in \mathcal{R}^{3 \times L} \tag{9}$$

$$\lambda_{ij} = [\lambda_{ij}^1, \ldots, \lambda_{ij}^L]^T \in \mathcal{R}^{L \times 1} \tag{10}$$

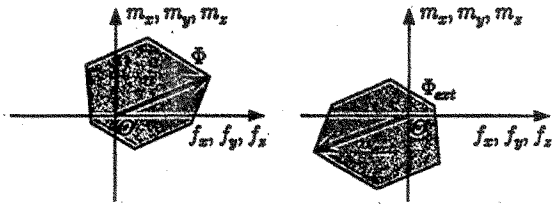

(a) Space $\Phi \ni O$ (b) External force space Φ_{ext}

Fig.4 Convex polygon spanned by Φ

where L is the number of faces of polyhedral convex cone as shown in Fig.3(b). Applying eqs.(4) and (8) to m fingers, we get

$$\tau = J^{\mathrm{T}} f \tag{11}$$

$$f = V\lambda \tag{12}$$

$$\lambda \geq \mathbf{o} \tag{13}$$

where

$$\tau = \left[\tau_1^{\mathrm{T}}, \ldots, \tau_m^{\mathrm{T}}\right]^T \in \mathcal{R}^{mn \times 1} \tag{14}$$

$$J^{\mathrm{T}} = \begin{bmatrix} J_1^{\mathrm{T}} & & \\ & \ddots & \\ & & J_m^{\mathrm{T}} \end{bmatrix} \in \mathcal{R}^{nm \times 3\Sigma k_i} \tag{15}$$

$$f = \left[f_1^{\mathrm{T}}, \ldots, f_m^{\mathrm{T}}\right]^{\mathrm{T}} \in \mathcal{R}^{3\Sigma k_i \times 1} \tag{16}$$

$$V = \begin{bmatrix} V_1 & & \\ & \ddots & \\ & & V_m \end{bmatrix} \in \mathcal{R}^{3\Sigma k_i \times L\Sigma k_i} \tag{17}$$

$$V_i = \begin{bmatrix} V_{i1} & & \\ & \ddots & \\ & & V_{ik_i} \end{bmatrix} \in \mathcal{R}^{3k_i \times Lk_i} \tag{18}$$

$$\lambda = \left[\lambda_1^{\mathrm{T}}, \ldots, \lambda_m^{\mathrm{T}}\right]^{\mathrm{T}} \in \mathcal{R}^{L\Sigma k_i \times 1} \tag{19}$$

$$\lambda_i = \left[\lambda_{i1}^{\mathrm{T}}, \ldots, \lambda_{ik_i}^{\mathrm{T}}\right]^T \in \mathcal{R}^{Lk_i \times 1} \tag{20}$$

By deleting f from eqs.(11) and (12), we finally obtain

$$\tau = J^{\mathrm{T}} V \lambda \tag{21}$$

3.3 Basic behaviour under constant torque commands

In both lifting and grasping phases, we apply constant torque commands to each joint. Such a control scheme releases us from computing the exact contact forces as well as the exact object's position, since they are naturally determined by the combination among the command torque, the object's weight and the geometrical relationship. Under the constant torque control, eq.(21) results in mn equations for $L\Sigma_{i=1}^m k_i$ unknown variables λ. Generally, the number of unknown variables is greater than that of equations, and as a result,

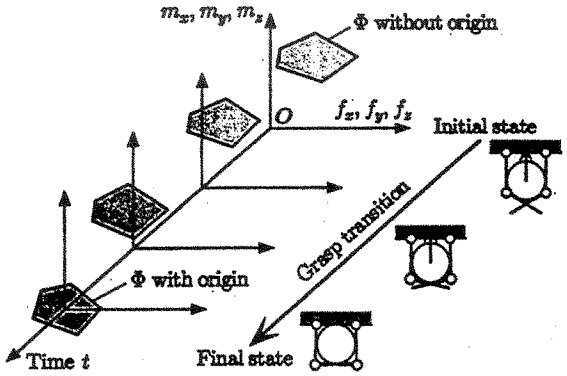

Fig.5 Grasp transition with Φ

there exist infinite combinations of contact forces satisfying eq.(21) for a set of torque command. It is well known [5] that the resultant force f_o and moment m_o span a convex polygon Φ as shown in Fig.4(a), where u_o is a 6D vector given by

$$u_o = \begin{bmatrix} f_o \\ m_o \end{bmatrix} = \begin{bmatrix} \sum_{i=1}^{m}\sum_{j=1}^{k_i} f_{ij} + Mg \\ \sum_{i=1}^{m}\sum_{j=1}^{k_i} \{(p_{ij} - r_G) \times f_{ij}\} \end{bmatrix} \quad (22)$$

where M, r_G, and g denote the mass of object, the position vector of the center of gravity of the object, and the gravitational vector, respectively. If Φ includes the origin O as shown in Fig.4(a), the commanded torque can generate at least one set of contact forces making $u_o = 0$, which means that the object will stop at the equilibrium point. Now, suppose that the object is stationary, and external force and moment vector u_{ext} is applied to the object. In such a case, the robot finger can automatically generate contact forces which can resist to u_{ext} without changing the joint torque. The space Φ_{ext} spanned by u_{ext} is determined such that the following relationship can be satisfied

$$u_o + u_{ext} = o \quad (23)$$

The vector space Φ_{ext} is called Admissible External Force Space [5] whose size can be an index for evaluating the robustness of enveloping grasp.

3.4 Sliding condition

In our work, the torque command in the lifting phase should be determined, such that Φ may exclude the origin O as shown in Fig.5. Since Φ spans a convex polygon, the resultant force has the minimum and the maximum components for each axis. Therefore, by examining the maximum and the minimum values in a particular direction, we can evaluate whether the object moves in the direction or not. For example, if both have the positive signs in a particular direction, the sliding motion to the positive direction is guaranteed. As for a sliding motion of enveloped object, the following theorem exists.

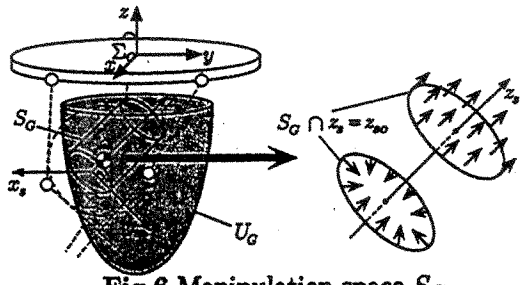

Fig.6 Manipulation space S_G

Theorem 1 *Consider * directional sliding motion of object for a fixed center of gravity of object.*

(i) If $\{f_*^{min}\}^{min} \cdot \{f_*^{max}\}^{max} > 0$, *it is guaranteed that the object slides to the* sgn $[\{f_*^{min}\}^{min}]$ *direction of * axis. (A sufficient condition leading to sliding in * direction)*

(ii) If $\{f_*^{min}\}^{min} \cdot \{f_*^{max}\}^{max} \leq 0$, *the object motion in the specified direction is not uniquely determined,*
where sgn$[v] = +1$ *for* $v \geq 0$ *and* sgn$[v] = -1$ *for* $v < 0$, *and* f_*^{min} *and* f_*^{max} *denote the minimum and the maximum values in the * direction, respectively, and* $\{\ \}^{min}$ *and* $\{\ \}^{max}$ *denote the minimum and the maximum values for all possible orientations of the object, respectively.*

Proof: (omit) ■

4 Transition Stability [9]

Let $p_G = (x_G, y_G, z_G)^T$ be the gravitational center. To avoid multiple finger postures for a given gravitational center p_G, we assume that the swing d.o.f of each finger is fixed. Under this assumption, let us now define the transition stability following after an idea of virtual pipe.

Definition 1 *Let* Σ_s *be a coordinate system, where* z_s *axis is chosen such that it may coincide with the direction of the goal. Virtual pipe* S_G *is defined by (i)* $S_G \subset U_G$ *where* U_G *is the space spanned by* p_G. *(ii)* S_G *forms a cylindrical shape, where the section at* $z_s = 0$ *is the initial position of object and the other section is the goal.*

Definition 2 *The transition stability is guaranteed in* S_G *if the following two conditions hold in* $z_{ss} \leq z_{so} \leq z_{sf}$, *irrespective of the orientation of object.*

(i) For the circular cross section $z_s = z_{so}$, $\{(t^T f_0)^{min}\}^{min} > 0$ *for the positive goal* $\{(t^T f_0)^{max}\}^{max} < 0$ *for the negative goal where* t *is the unit vector expressing the* z_s *axis.*

(ii) For the boundary of circular cross section $z_s = z_{so}$, $\{(n^T f_0)^{max}\}^{max} > 0$ *and* $\{(n^T f_0)^{min}\}^{min} > 0$ *where* n *is an inward normal unit vector at the boundary.*

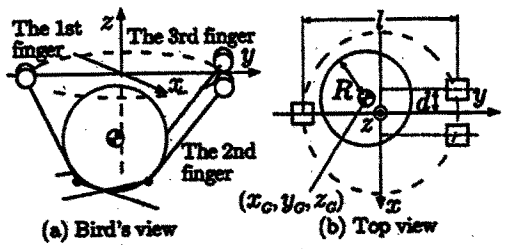

Fig.7 Simulation model for a sphere object

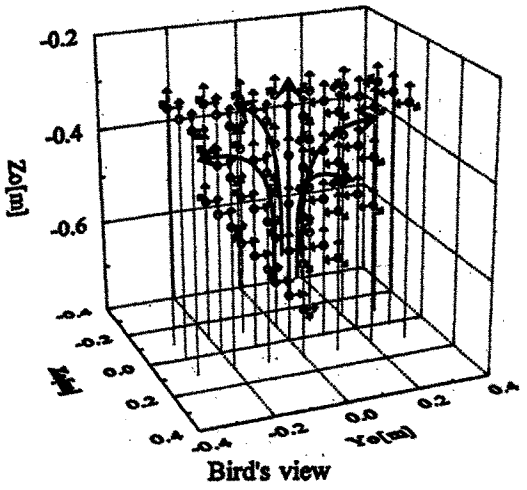

Fig.8 Force flow diagram for a sphere object ($l = 1.0$[m], $d = 0.05$[m], $R = 0.2$[m], $Mg = -1$[N] and $\alpha = \pi/18$[rad])

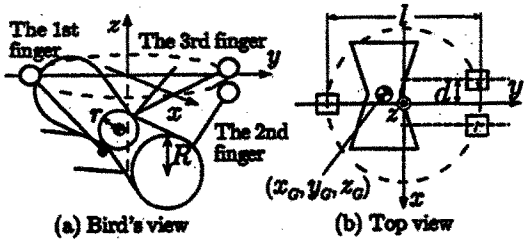

Fig.9 Simulation model for a tsuzumi object

5 Force-Flow-Diagram

In this section, we introduce the force-flow-diagram as a tool for judging whether the transition stability is confirmed under the torque command or not. We define a new coordinate system Σ_1 for force-flow-diagram. Based on theorem 1, we now define the force-flow and the force-flow-diagram as follows.

Definition 3 *Let* $*$ *be* x_1, y_1, *and* z_1 *axis, respectively.*

(i) If $\{f_*^{min}\}^{min} \cdot \{f_*^{max}\}^{max} > 0$, *we put an arrow at* p_G *in* $\mathrm{sgn}\,[\{f_*^{min}\}^{min}]$ *direction in* $*$ *axis.*

(ii) If $\{f_*^{min}\}^{min} \cdot \{f_*^{max}\}^{max} \leq 0$, *we put* $\circ$.

We call the arrow or $\circ$ the force-flow. We also call the map displaying the force-flow at various position of the center of gravity of object the force-flow-diagram. A big advantage to utilize this diagram is that we can roughly estimate the object's behaviour without solving a set of differential equations with respect to time.

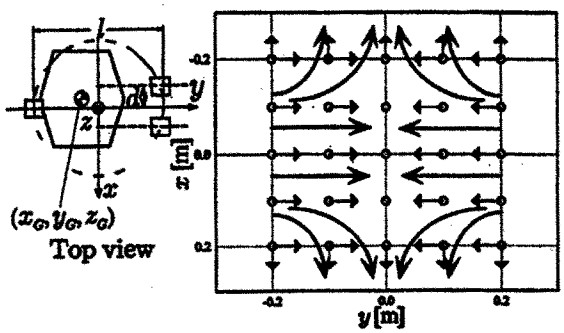

Fig.10 Force flow diagram for $N = 40$, $l = 1.0$[m], $d = 0.05$[m], $R = 0.2$[m], $r = 0.3$[m], $Mg = -1$[N] and $\alpha = \pi/18$[rad]

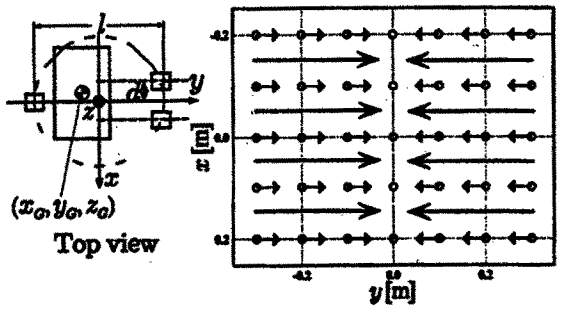

Fig.11 Force flow diagram for $N = 40$, $l = 1.0$[m], $d = 0.05$[m], $R = 0.2$[m], $r = 0.2$[m], $Mg = -1$[N] and $\alpha = \pi/18$[rad]

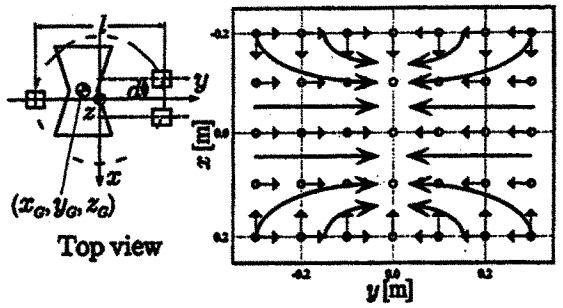

Fig.12 Force flow diagram for $N = 40$, $l = 1.0$[m], $d = 0.05$[m], $R = 0.2$[m], $r = 0.1$[m], $Mg = -1$[N] and $\alpha = \pi/18$[rad]

6 Simulations

A three fingered hand is assumed as shown in Fig.7, where each finger is fixed at the palm. Fig.8 shows the force-flow-diagramfor a sphere object, where $l = 1.0$[m], $d = 0.05$[m], $R = 0.2$[m], $Mg = -1$[N], and $\alpha = \pi/18$[rad], respectively. An interesting observation in Fig.8(b) is that the object placed with a bit shift from x axis receives a force, such that it may always push the object away from the axis, which means that the object is easily dropped from the hand during the lifting

phase, while the force flow shows a stable behaviour in the side view. Since S_G satisfying (ii) in the transition stability in the lifting phase can not be found in U_G, the transition stability is not guaranteed for a sphere.

Fig.9 shows simulation model for a tsuzumi object, where the object's shape is characterized by two parameters, R and r. For example,if $R = r$, the object's shape results in cylindrical shape, For $R > r$ and $R < r$, the shape becomes concave and convex,respectively.

Fig.10 shows the top view of the force-flow diagram for $R < r$. Since the side view of the force-flow diagram is similar to that obtained for a sphere, we simply omit it for the space limitation. It can be seen from Fig.10 that, for a convex object, the force-flow diagram shows an unstable behavior. Fig.11 shows the top view of the force-flow diagram for $R = r$ (cylindrical object). For such an object, it seems to be a critical behavior, where we can not clearly specify whether the z-directional force results in positive or negative.

Fig.12 shows the top view of the force-flow diagram for $R > r$. For such an object, we can observe that the object whose center of gravity is placed in an arbitrary point always moves toward $y = 0$ without moving away from the boundary. This is a stable behaviour. Totally judging, we have a tendency in which the lifting phase becomes stably for a concave object, while it becomes unstable for a convex one.

7 Conclusions

The main results obtained in this work are as follow:

(1) We showed a sufficient condition for sliding an object enveloped by a multi-fingered robot hand.
(2) We provided a general definition on the transition stability for an object enveloped by a multi-fingered robot hand.
(3) As a tool for evaluating the transition stability, we introduced the force-flow-diagram.
(4) Through simulations, we showed that the lifting phase in concave objects can be achieved stably, while that for convex objects tends to be unstable.

This work was supported by the Inter University Robotics Project funded by the Ministry of Education. Finally, I would like to express my sincere thanks to Mr. M. Takeshita, Mr. K. Furutera, Mr. N. Thaiprasert and Mr. Y. Hino for their cooperation in this work.

References

[1] Mirza, K. and D. E. Orin, "Control of force distribution for power grasp in the DIGITS system", *Proc. of the IEEE 29th CDC Conf.*, pp.1960–1965, 1990.

[2] Bicchi, A., "Force distribution in multiple whole-limb manipulation", *Proc. of the IEEE Int. Conf. on Robotics and Automation*, pp.196–201, 1993.

[3] Omata, T. and K. Nagata, "Rigid body analysis of the indeterminate grasp force in power grasps", *Proc. of the IEEE Int. Conf. on Robotics and Automation*, pp.1787–1794, 1996.

[4] Zhang, X, Y. Nakamura, K. Goda and K. Yoshimoto, "Robustness of power grasp", *Proc. of the IEEE Int. Conf. on Robotics and Automation*, pp.2828–2835, 1994.

[5] Zhang, X, Y. Nakamura and K. Yoshimoto: "Mechanical Analysis of Grasps with Defective Contacts Using Polyhedral Convex Set Theory", *Journal of the Robotics Society of Japan*, Vol. 14, No. 1, pp. 105–113, 1996.(in Japanese)

[6] Kaneko, M., Y. Tanaka and T. Tsuji, "Scale-dependent grasp", *Proc. of the IEEE Int. Conf. on Robotics and Automation*, pp.2131–2136, 1996.

[7] M. Kaneko, Y. Hino, T. Tsuji: "On Three Phases for Achieving Enveloping Grasps", *Proc. of the 1997 IEEE Int. Conf. on Robotics and Automation*, 1997 (to appear).

[8] Kaneko. M, N. Thaiprasert, T. Tsuji: "Experimental approach on enveloping grasp for column objects", *Preprints of 5th Int. Symp. on Exp. Robotics*, pp.17-29, 1997.

[9] M. Kaneko, M. Higashimori and T. Tsuji: "Transition stability of enveloped objects", *Proc. of the 1997 IEEE Int. Conf. on Robotics and Automation, Leuven*, 1998 (to appear).

[10] Jeannerod, M., "Attention and performance, chapter Intersegmental coordination during reaching at natural visual objects", pp.153–168, Erlbaum, Hillsdale, 1981.

[11] Bard, C. and J. Troccaz, "Automatic preshaping for a dexterous hand from a simple description of objects", *Proc. of the IEEE Int. Workshop on Intelligent Robots and Systems*, pp.865–872, 1990.

[12] Trinkle, J. C. and R. P. Paul, "The initial grasp liftability chart", *Trans. on Robotics and Automation*, Vol.5, No.1, pp.47–52, 1989.

[13] Trinkle, J. C., J. M. Abel and R. P. Paul, "Enveloping, frictionless planar grasping", *Proc. of the IEEE Int. Conf. on Robotics and Automation*, 1987.

[14] Salisbury, J. K., "Whole-Arm manipulation", *Proc. of the 4th Int. Symp. of Robotics Research*, Santa Cruz, CA, 1987. Published by the MIT Press, Cambridge MA.

[15] Rimon, E. and A. Blake, "Caging 2D bodies by 1-parameter two-fingered gripping systems", *Proc. of the IEEE Int. Conf. on Robotics and Automation*, pp.1458–1464, 1996.

[16] Kleinmann, K. P., J. Henning, C. Ruhm and H. Tolle, "Object manipulation by a multi-fingered gripper: On the transition from precision to power grasp", *Proc. of the IEEE Int. Conf. on Robotics and Automation*, pp.2761–2766, 1996.